

Probing Charge Transport of Ruthenium-Complex-Based Molecular Wires at the Single-Molecule Level

Ke Liu,^{†,*} Xianhong Wang,^{†,*} and Fosong Wang[†]

[†]State Key Laboratory of Polymer Physics and Chemistry, Changchun Institute of Applied Chemistry, Chinese Academy of Sciences, Changchun 130022, People's Republic of China, and ^{*}Graduate School of the Chinese Academy of Science, Beijing 100039, People's Republic of China

The core field of molecular electronics is to understand and control nanoscale charge transport. A promising approach for this purpose is to trap few molecules or even a single molecule between two nanoscale-separated electrodes, namely, "molecular junctions".^{1–3} Significant progress, including the measurement^{2,4} and modeling^{1,3} of charge transport in molecular junctions, has been made to reveal the underlying charge transport mechanism. Unfortunately, almost all of the molecular wires obey a length-dependent charge transport rule,³ which originates from the energy mismatch between the molecular orbitals and the electrode Fermi level and is considered to hamper the long-range charge transport of molecular wires. To tackle this problem, transition metal complexes containing π -conjugated molecular wires have been proposed,^{5–8} due to their capability of modulating the electronic band structure. For instance, a strong coupling between metal fragments along the π -conjugated backbone was observed due to the incorporation of ruthenium complex,⁵ and a weak dependence of molecular conductance on molecular length was found in ruthenium(II) bis(σ -arylacetylide) complexes.⁸ Although

ABSTRACT A ruthenium(II) bis(σ -arylacetylide)-complex-based molecular wire functionalized with thiolacetyl alligator clips at both ends (OPERu) was used to fabricate gold substrate–molecular wire–conductive tip junctions. To elucidate the ruthenium-complex-enhanced charge transport, we conducted a single-molecule level investigation using the technique-combination method, where electronic decay constant, single-molecular conductance, and barrier height were obtained by scanning tunneling microscopy (STM) apparent height measurements, STM break junction measurements, and conductive probe-atomic force microscopy (CP-AFM) measurements, respectively. A quantitative comparison of OPERu with the well-studied π -conjugated molecular wire oligo(1,4-phenylene ethynylene) (OPE) indicated that the lower electronic decay constant as well as the higher conductance of OPERu resulted from its lower band gap between the highest occupied molecular orbital (HOMO) and the gold Fermi level. The small offset of 0.25 eV was expected to be beneficial for the long-range charge transport of molecular wires. Moreover, the observed cross-platform agreement proved that this technique-combination method could serve as a benchmark for the detailed description of charge transport through molecular wires.

KEYWORDS: ruthenium-complex-enhanced charge transport · scanning tunneling microscopy · conductive probe-atomic force microscopy · technique-combination method · electronic decay constant · single molecular conductance · barrier height

such findings are encouraging, the reasonable interpretation of the ruthenium-complex-enhanced charge transport phenomenon remains an open question.

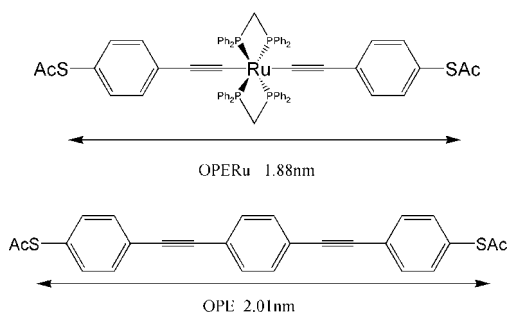
The ability of STM to study molecular wires at molecular resolution provides an unprecedented insight into how individual molecules function as active electronic components.⁹ Generally, there are three important factors dominating the electrical property of molecular junctions: electronic decay constant β , single molecular conductance, and barrier height. Weiss and co-workers isolated individual molecules in an alkanethiol matrix^{10,11} and assessed their electronic decay constant β by a two-layer tunnel junction model.¹² Xu *et al.* reported a reproducible method to form a large amount of molecular junctions,¹³ by which single molecular conductance was

*Address correspondence to xhwang@ciac.jl.cn.

Received for review June 16, 2008 and accepted October 15, 2008.

Published online November 4, 2008. 10.1021/nn800475a CCC: \$40.75

© 2008 American Chemical Society



Scheme 1. Structures and computed molecular lengths of molecular wires studied in this work.

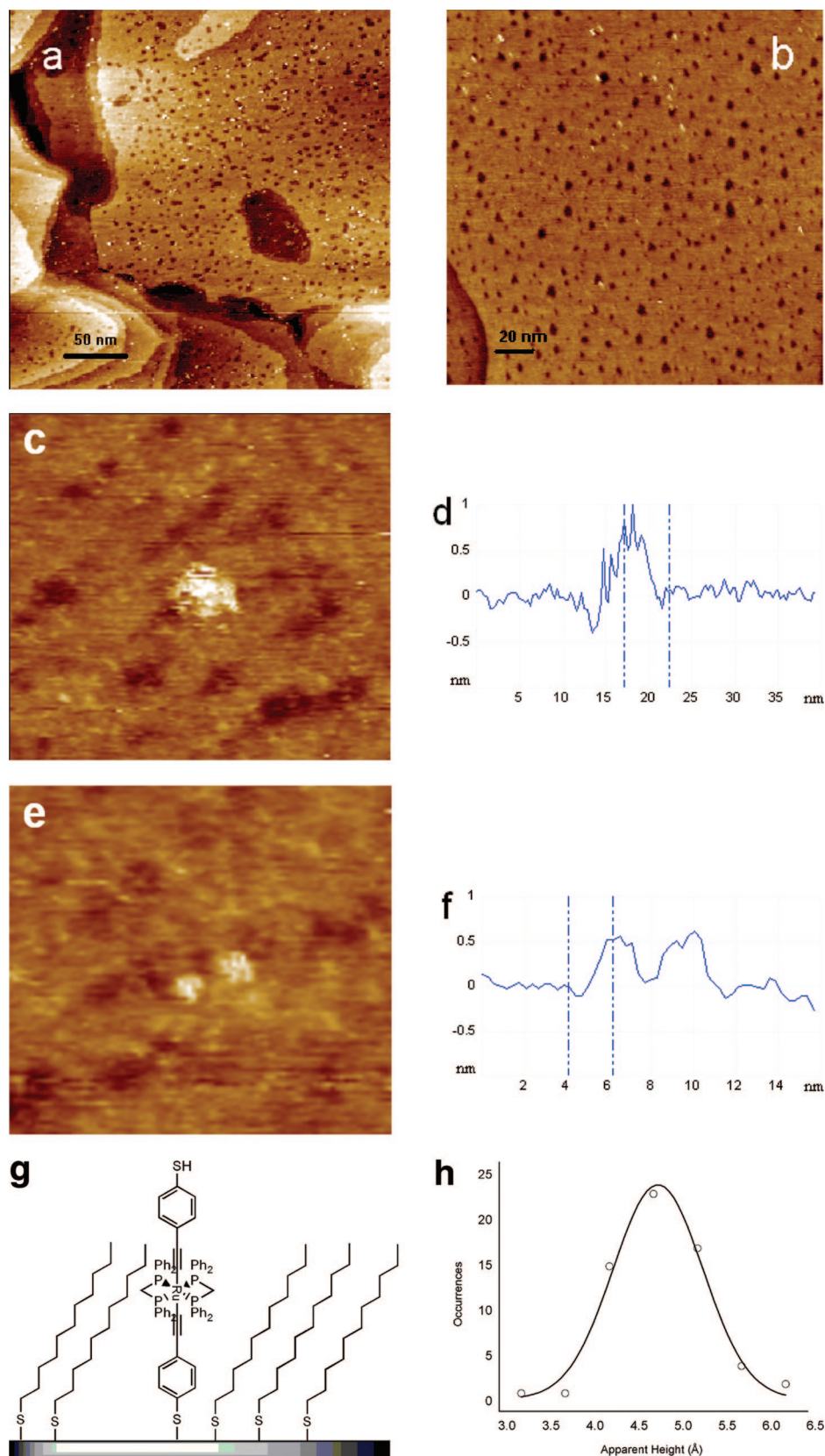


Figure 1. (a) Constant current STM topography ($I = 2$ pA, $V = 1$ V) of **OPERu** inserted into the decanethiol matrix. Scanning size: 325×325 nm². The inserted molecules appeared as the bright spots in the image. (b) A 200×200 nm² topography of the mixed SAM. (c) A zoom-in image with the scanning size of 35×35 nm². (d) Cross-section analysis of the bright spot in (c). (e) A zoom-in image with the scanning size of 20×20 nm². (f) Cross-section analysis of the bright spots in (e). (g) A cartoon illustration of a single **OPERu** molecule inserted into the decanethiol matrix. (h) Statistical analysis of the measured apparent heights of **OPERu** on the basis of 70 insertion events. The bin size was 0.5 Å. The data were fitted by Gaussian function.

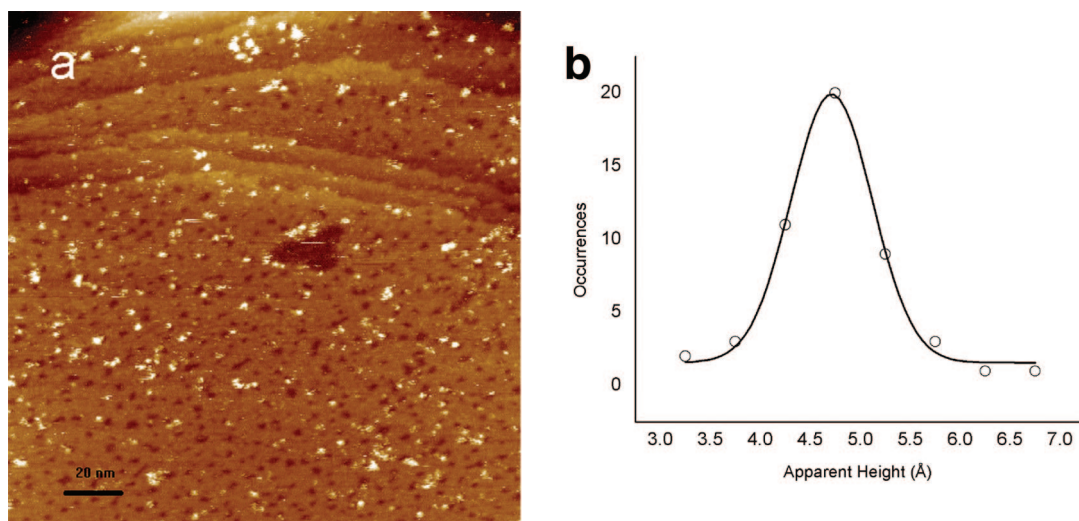


Figure 2. (a) Constant current STM topography ($I = 3$ pA, $V = 1$ V) of **OPE** inserted into the decanethiol matrix. Scanning size of 200×200 nm². (b) Statistical analysis of the measured apparent heights of **OPE** on the basis of 50 insertion events. The bin size was 0.5 Å. The data were fitted by Gaussian function.

obtained statistically. Beebe *et al.* found a transition from direct tunneling to field emission in π -conjugated thiols, and the voltage at which the transition occurs could be regarded as a measure of the barrier height.¹⁴ Since each of these methods describes molecular junctions from a different point of view, a combination of different techniques may be a choice to gain a complete understanding.¹⁵ Therefore, this paper is focused on two issues, one is to elucidate the factors dominating the ruthenium-complex-enhanced charge transport, and the other is to present a methodology for the precise determination of critical parameters affecting charge transport.

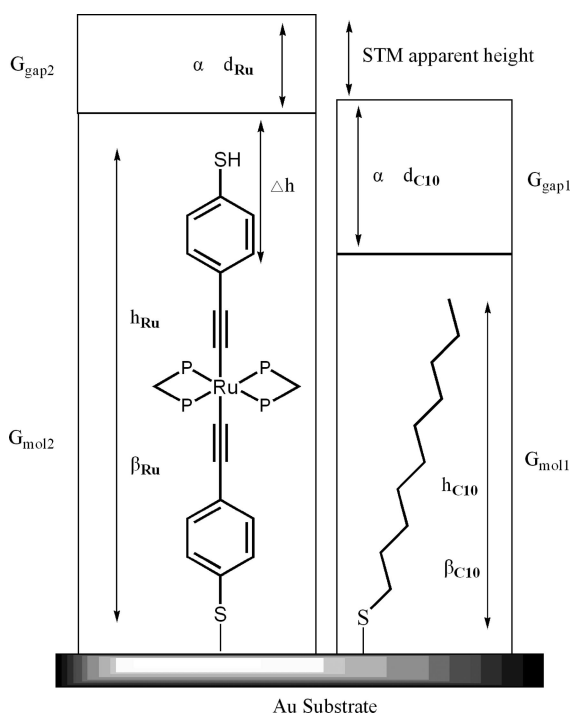
To that end, molecular wire **OPERu** (Scheme 1) was used to fabricate gold substrate–molecular wire–conductive tip junctions, where electronic decay constant, single molecular conductance, and barrier height were obtained by STM apparent height measurements, STM break junction measurements, and CP-AFM measurements, respectively. Further, the interplay among these three parameters will be intensively discussed, and the feasibility of using this technique-combination method to provide the detailed information of the ruthenium-complex-enhanced charge transport will also be demonstrated.

RESULTS AND DISCUSSION

STM Apparent Height Measurements for Electronic Decay Constant

Constant. STM images were recorded in the constant current mode under ambient conditions, and high impedances (300 G Ω or higher) were chosen to ensure that the STM tip was above the mixed self-assembled monolayer (SAM). Figure 1a illustrates a typical topography of **OPERu** inserted into the decanethiol SAM matrix, and the bright spots reflect the presence of **OPERu**. As shown in Figure 1b, it was clearly seen from the topography that the inserted conjugated molecules **OPERu**

tended to adsorb nearby the etched-pits, which were caused by the Au surface re-formation during the self-assembly process.¹⁶ As depicted in Figure 1c, **OPERu** was protruding above the decanethiol matrix. This protrusion feature of **OPERu** was mainly due to its higher conductivity compared with the decanethiol SAM matrix, which could be quantified with apparent height. Figure 1d was the cross-section analysis of the bright spot in Figure 1c, giving the apparent height of ~ 0.7 nm and the lateral size of ~ 5 nm. The lateral sizes of



Scheme 2. Two-layer tunnel junction model. The h and d were the layer thicknesses, α and β were the tunneling decay constants, and G_{gap} and G_{mol} were the conductance of the gap and molecule, respectively. Δh is the measured apparent height difference, and Δh is the calculated physical height difference.

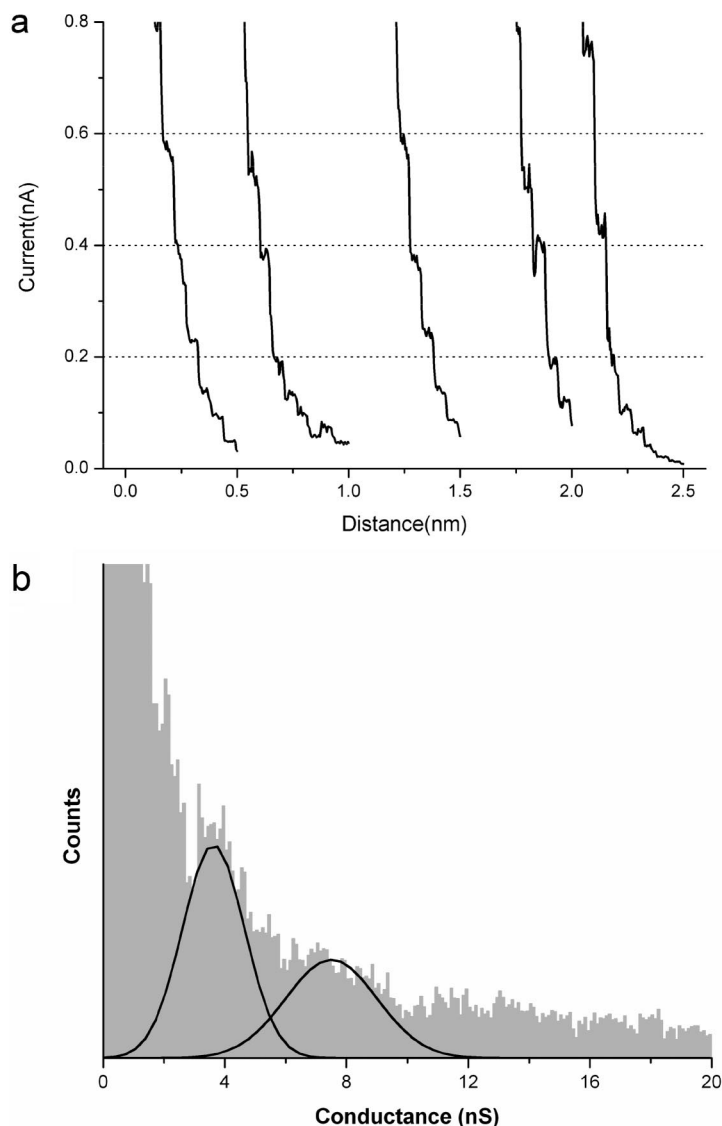


Figure 3. (a) Traces of current versus traveling distance for **OPE** recorded at -50 mV. (b) Conductance histogram based on 328 $I-S$ traces.

bright spots typically ranged from 2 to 5 nm according to our observation, and each bright spot could be attributed to a single molecule or a small bunch of molecules, depending on its lateral size. For example, two bright spots in Figure 1e with lateral sizes of ~ 2 nm had apparent heights of ~ 0.5 nm. We tentatively attributed each bright spot in Figure 1e to a single **OPERu** molecule, while the bright spot in Figure 1c corresponded to a small bunch of **OPERu** molecules. Thus, bright spots with relatively smaller lateral sizes were selected for the cross-section analysis to yield the apparent heights of single **OPERu** molecules. It is worth noting that both **OPERu** and **OPE** displayed stochastic switching,^{17–19} which was a random phenomenon manifested as inserted molecules that blinked on and off (Figures S1 and S2 in Supporting Information). Due to the fluctuation of the measured apparent heights, the distribution of the measured apparent heights of

OPERu was plotted on the basis of a statistical analysis of 70 insertion events. As shown in Figure 1h, the measured apparent heights ranged from 3 to 6.5 Å in a Gaussian distribution. Therefore, the apparent height of **OPERu** was determined as 4.8 ± 1.0 Å using Gaussian fitting. As a reference, the topography of **OPE** inserted into the decanethiol SAM matrix was recorded and is shown in Figure 2a. In contrast with **OPE**, a relative smaller density of **OPERu** was observed from topographies, which could be attributed to the hindered effect caused by the ligands in **OPERu**. As shown in Figure 2b, on the basis of 50 insertion events, the apparent height of **OPE** was determined as 4.7 ± 0.8 Å, which was consistent with previous reports.^{10,11,17}

As first developed by Bumm *et al.*,¹² the method of using the STM apparent height to determine the electronic decay constant β of π -conjugated molecules has been successfully utilized to correlate the electronic transmission property with molecular structure. Poulsen *et al.* systematically investigated the effect of conjugation path on the electronic transport through single oligo(phenylene vinylene) molecule.²⁰ Blum *et al.* observed a significant change in the electronic decay constant β due to the incorporation of a ruthenium fragment at the end of OPE molecular wire.⁷ As shown in Scheme 2, a simple two-layer tunnel junction model^{7,12,15,20,21} was used to relate the STM apparent height of the inserted molecule to its electronic decay constant β . In this two-layer model, the transconductance (G) of each layer was $G = G_0 \exp(-\beta h)$, where G_0 was the contact conductance, β was the electronic decay constant, and h was the layer thickness. Since STM was operated in the constant current mode, thus $G_{\text{gap}1}G_{\text{mol}1} = G_{\text{gap}2}G_{\text{mol}2}$. Assuming that the tunneling property of the air gap and the contact conductance were the same for both molecule fragments, the electronic decay constant of the inserted molecule was solved through a simple mathematical deduction, $\beta_{\text{Ru}} = [\beta_{\text{C10}}h_{\text{C10}} - \alpha(\Delta\text{STM} - \Delta h)]/h_{\text{Ru}}$, where ΔSTM was the measured apparent height difference, Δh was the calculated physical height difference, and α was the decay constant of air with a value of 2.3 \AA^{-1} . The electronic decay constant β for alkanethiols has been determined as 1.2 \AA^{-1} by electrochemistry,²² STM break junctions,²³ as well as CP-AFM,²⁴ and it serves as a reference for evaluating the conductivity of inserted conjugated molecules. Therefore, the electronic decay constant β of **OPERu** was $1.01 \pm 0.25 \text{ \AA}^{-1}$, determined from the two-layer tunnel junction model, while it was $1.11 \pm 0.18 \text{ \AA}^{-1}$ for **OPE**. For **OPE**, an agreement with reported values of the electronic decay constant β ^{7,20} determined by STM was observed. It should be noted that the electronic decay constant β of **OPE** determined by STM was much larger than that determined by CP-AFM. This discrepancy originates from the difference in the operational principle between STM and CP-AFM. For STM, the determined electronic decay constant β

is a relative value using the insulating alkanethiols as the reference, and an air gap lies between the STM tip and SAM. For CP-AFM, the determined electronic decay constant β is an absolute value obtained from the semilog plot of molecular resistances *versus* repeated units, and the conductive tip is in direct contact with SAM.

The difference of 0.1 \AA^{-1} in electron decay constant β between **OPE** and **OPeRu** was as much as the difference between **OPE** and decanethiol. Numerically, **OPeRu** would be 6 times more conducting than **OPE**. So, one can predict that the incorporation of ruthenium complex would enhance molecular conductance more remarkably for longer molecular wires. However, a low β is a necessary but not sufficient condition for high conductance of molecular wires. Therefore, single molecular conductance measurements were needed for a direct comparison between **OPE** and **OPeRu**.

STM Break Junction Measurements for Single Molecular Conductance. As shown in Figures 3a and a, current–distance ($I-S$) traces displayed a typical stepwise feature with the stretched length of ~ 0.05 nm. On the basis of at least 300 successful pull-off processes out of thousands of repeated measurements, conductance histograms were constructed statistically. As shown in Figures 3b and b, conductance histograms revealed well-defined peaks at integer multiples of a fundamental conductance value, which was used to identify the single molecular conductance. As a result, the single molecular conductances of **OPE** and **OPeRu** were determined as 3.6 ± 2.0 and 19 ± 7 nS, respectively. As a reference, the experimental single molecular conductance of molecules analogous to **OPE** ranged from 2 to 13 nS.^{25–27}

As expected, **OPeRu** was more conducting than **OPE**. However, the shorter molecular length of **OPeRu** (1.88 nm) as compared with **OPE** (2.01 nm) may also lead to higher conductance. Assuming that molecular length was the only factor affecting molecular conductance, the single molecular conductance of **OPeRu** would be 6 nS using a β value of 0.21 \AA^{-1} .²⁸ Therefore, apart from the molecular length, the structure of backbone did play an important role in molecular conductance for **OPeRu**. This experimental observation was consistent with the prediction in the above section. In contrary, a break junction investigation reported by Mayor *et al.* indicated that *trans*-platinum(II) bis(σ -arylacetylide) complex acted as an insulator.²⁹ This discrepancy should be related to the difference in the nature of the metal–acetylene bond between these two systems³⁰ since the platinum–acetylene bond has hardly any π character separating the molecular rod into two independent conjugated systems,²⁹ whereas the ruthenium–acetylene bond has high electron mobility delocalizing the backbone.^{5,7,8} Therefore,

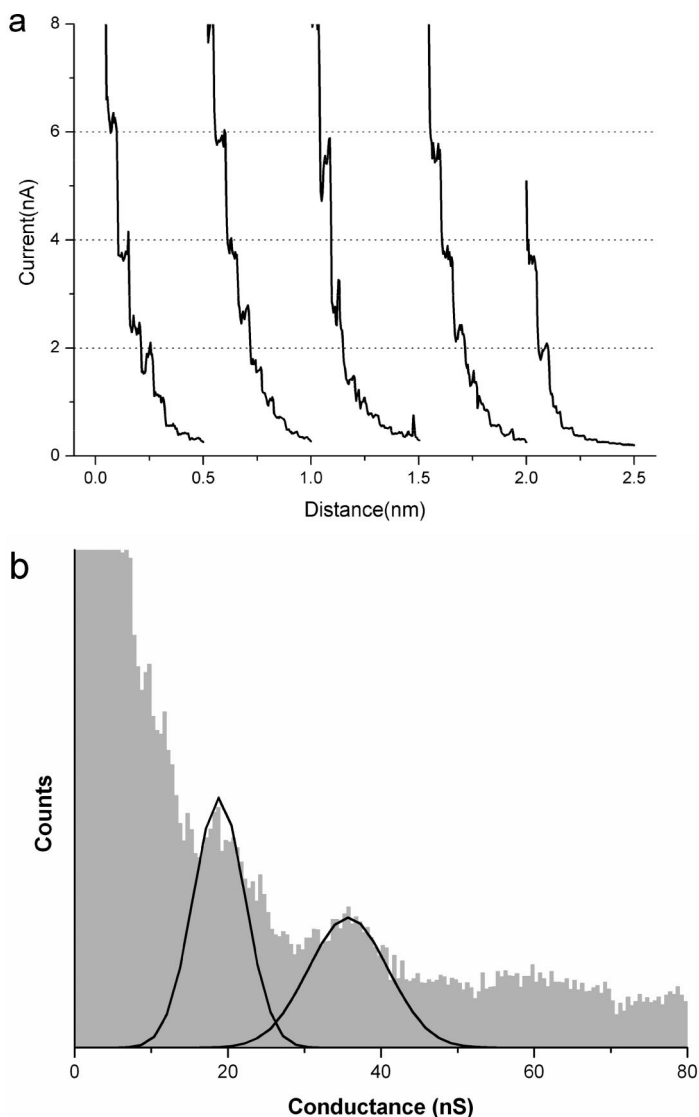


Figure 4. (a) Traces of current *versus* traveling distance for **OPeRu** recorded at -100 mV. (b) Conductance histogram based on 350 $I-S$ traces.

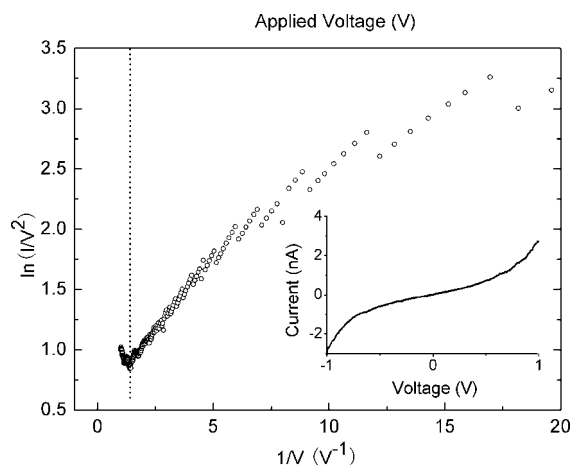
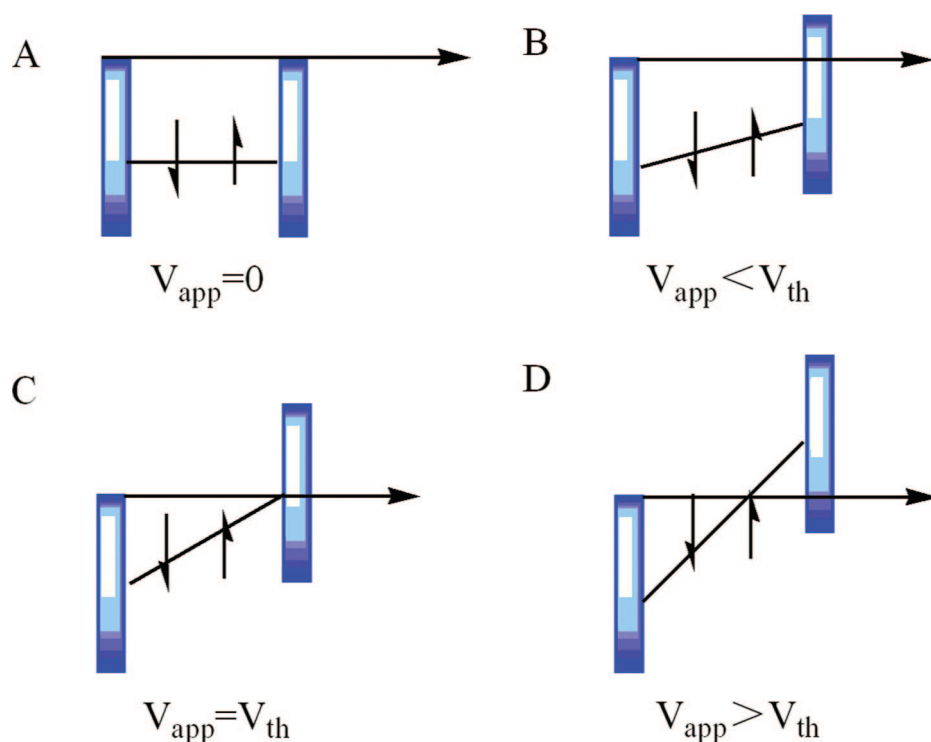


Figure 5. Plot of $\ln(I/V^2)$ *versus* $\ln(1/V)$ for **OPE**. Circles were the average of 10 current–voltage curves for the Au–**OPE**–PtTi junction by CP-AFM. The dashed line corresponds to the voltage (V_{th}) at which the tunneling barrier transition from trapezoidal to triangular occurred. The inset shows current–voltage data.



Scheme 3. Cartoon for the transition from trapezoidal barrier to triangular barrier. The scheme was drawn for HOMO-mediated hole tunneling; V_{th} was the voltage at which the transition occurred, and V_{app} was the applied voltage. (A) represented the rectangular barrier, (B) represented the trapezoidal barrier, (C) represented the transition from trapezoidal barrier to triangular barrier, and (D) represented the triangular barrier.

we could conclude that the incorporation of ruthenium complex into the backbone may be a potential choice for constructing long molecular wires with high conductance.

To further understand the ruthenium-complex-enhanced charge transport, a detailed description of how ruthenium complex functioned was given on the basis of the electronic band structure.

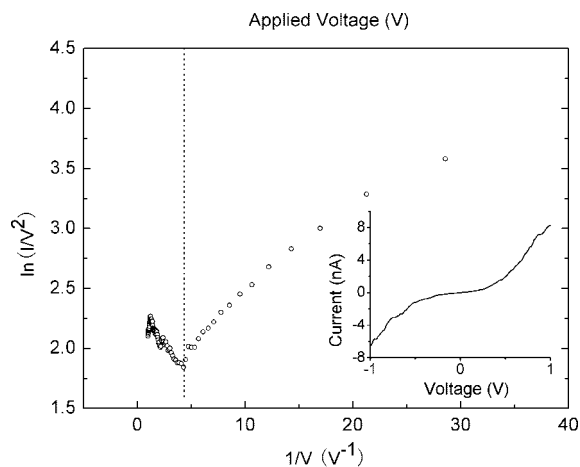


Figure 6. Plot of $\ln(I/V^2)$ versus $\ln(1/V)$ for **OPERu**. Circles represent the average of 10 current–voltage curves for the Au–**OPERu**–PtTi junction by CP-AFM. The dashed line corresponds to the voltage (V_{th}) at which the tunneling barrier transition from trapezoidal to triangular occurred. The inset shows current–voltage data.

CP-AFM Determination of Barrier Height and Molecular Orbital Calculation.

As shown in Scheme 3, when the applied bias is less than the barrier height, the dominant charge transport mechanism is direct tunneling represented by Simmons equation,³¹ where a trapezoidal barrier exists; when the applied bias exceeds the barrier height, the dominant charge transport mechanism is replaced by Fowler–Nordheim tunneling,³² where a triangular barrier exists. Experimentally, a transition from direct tunneling to Fowler–Nordheim tunneling was observed, corresponding to an inflection point appearing on the plot of $\ln(I/V^2)$ versus $\ln(1/V)$.¹⁴ The excellent linear correlation of the inflection point value (V_{th}) with the band gap between the metal Fermi level and the closest frontier molecular orbital suggested that this transition voltage could serve as a measure of the barrier height.

The plots of $\ln(I/V^2)$ versus $\ln(1/V)$ for **OPE** and **OPERu** are shown in Figures 5 and 6, respectively. Generally, a logarithmic increase corresponding to the direct tunneling mechanism appeared at low bias, and a linear decrease corresponding to the Fowler–Nordheim tunneling mechanism appeared at high bias.¹⁴ The value of barrier height was equal to the transition voltage. To verify the reproducibility, four supplemental measurements were performed for **OPE** and **OPERu** (Figures S3 and S4 in Supporting Information). The barrier heights along with their standard deviations for **OPE** and **OPERu** were determined as 0.66 ± 0.11 and 0.25 ± 0.03 eV, respectively. For **OPE**, a good agreement with recent reports was observed.^{14,33} For **OPERu**, Mahapatro *et al.* reported a quite consistent result using nanogap method during the preparation of this paper.³⁴ The different energy offsets had a substantial distinction in terms of charge transport. This evidence based on the electronic band structure supported our early argument that the incorporation of ruthenium complex into the backbone led to lower electronic decay constant β as well as higher conductance. Therefore, using a technique-combination method with good cross-platform agreement, a direct correlation between electronic decay constant β , single molecular conductance, and barrier height was revealed at the single-molecule level.

The UV–vis spectra, as shown in Figure 7, corresponded to band gaps of 3.69 and 3.46 eV for **OPE**

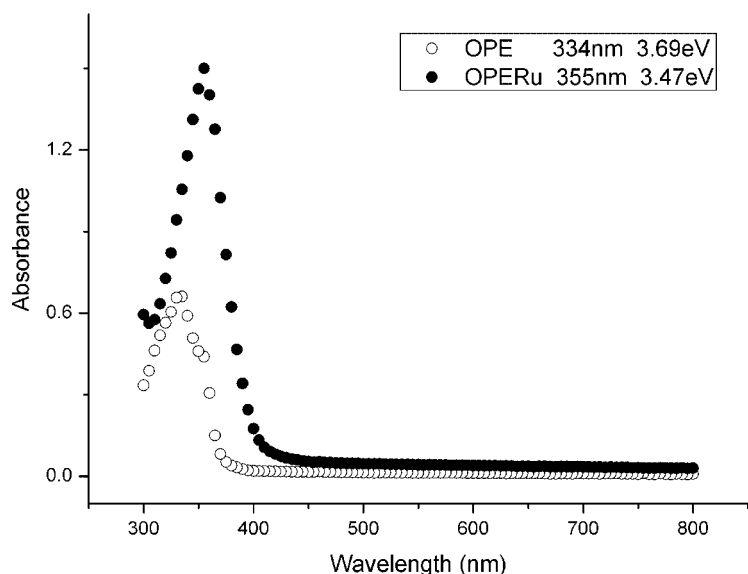


Figure 7. UV absorption spectra of **OPE** (○) and **OPERu** (●) in THF.

and **OPERu**, respectively, indicating that **OPERu** acted as a more efficient conductor due to its relatively lower HOMO–LUMO gap. The barrier height determination for **OPE** and **OPERu** indicated that the tunneling efficiency of **OPERu** across the molecular junction was enhanced due to its lower barrier height. However, there still lacked information of key importance: whether the LUMO or HOMO of **OPERu** was responsible for its lower barrier height. It has been widely accepted that charge transport in aromatic thiol systems is a HOMO-mediated process (hole tunneling).^{34–36} To address it, quantum chemistry calculations on **OPERu** along with **OPE** were performed within the density functional theory approximation. As shown in Figure 8, there was a remarkable distinction between the topologies of HOMO and LUMO of **OPERu**. The HOMO spanned the

entire length of the molecule, whereas the LUMO was localized in the ruthenium fragment. For **OPE**, the HOMO displayed a π feature, which was in contrast with the σ feature of the LUMO. Further, the calculated HOMO of **OPERu** nearly arrived at the gold Fermi level in energy, consistent with the barrier height results. Overall, for **OPERu**, the low barrier height between the HOMO and the gold Fermi level led to a low electron decay constant β and, consequently, high conductance.

SUMMARY

We have performed a single-molecule level investigation to elucidate the ruthenium-complex-enhanced charge transport through molecular wire **OPERu**. Using technique-combination method, we determined the electronic decay constant β , single molecular conductance, and barrier height by STM apparent height measurement, STM break junction measurement, and CP-AFM, respectively. By comparing with the well-studied π -conjugated molecular wire **OPE**, we asserted that the lower electronic decay constant β and the higher conductance of **OPERu** resulted from its lower band gap between the HOMO and the gold Fermi level. The small offset of 0.25 eV would be beneficial for the long-range charge transport of molecular wires. This is a key experimental evidence for the rational design of potential molecular wires with high conductance. Furthermore, the observed cross-platform agreement proved that the

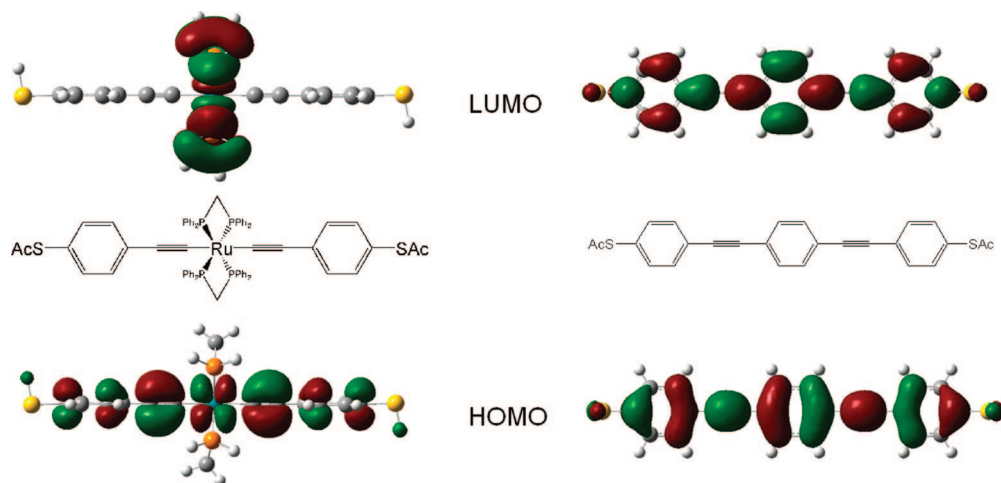


Figure 8. Electronic structures of **OPERu** and **OPE**. Quantum chemistry calculations were performed by density functional theory approximation³⁷ using the B3PW91 functional³⁸ coupled with the 6-311g(d,p) basis set³⁹ for **OPE** and the LANL2DZ basis set⁴⁰ for **OPERu** (phenyl groups in the ligands were replaced by hydrogen, considering computation consumption), respectively.

technique-combination method presented here could be proposed as a benchmark for the detailed description of charge transport through molecular

wires. Currently, the construction of functional molecular wires containing metal complex is ongoing in our laboratory.

MATERIALS AND METHODS

Materials. Tetrahydrofuran (THF) was distilled under nitrogen over sodium benzophenone ketyl. Other reagents and solvents were purchased from commercial suppliers and used without further purification. The synthesis of the molecular wires in Scheme 1 was similar to the earlier publication.²⁸

STM Apparent Height Measurements of Conjugated Molecules Inserted Decanethiol SAMs. The STM experiments were performed at room temperature under ambient atmosphere on a Digital Instruments (Santa Barbara, CA) Nanoscope 3A Multimode equipped with an A-scanner and low-current converter with a picoamp boost stage. Mechanically cut Pt–Ir tips (0.25 mm) were used. The bias voltage was 1 V, and set-point current was 2 pA. The Au{111} substrate on mica (Molecular Imaging, Phoenix, AZ) was annealed by hydrogen flame before SAM deposition; the host SAM was then prepared by immersing the Au substrate in a 1 mM solution of the decanethiol in ethanol for 24 h. The decanethiol SAM-modified Au{111} on mica was rinsed with ethanol ultrasonically and dried under a nitrogen stream. To make conjugated molecule wire inserted decanethiol SAMs, a 0.1 μ M THF solution of the molecular wire from Scheme 1 was prepared under nitrogen protection, and the thioacetyl group was deprotected by adding concentrated NH_4OH (5 μ L) and incubated for 10 min. The above decanethiol SAM-modified Au{111} on mica was immersed in the thioacetyl group deprotected molecular wire solution for 4 h, then rinsed by dry THF ultrasonically, dried under nitrogen stream, and finally the conjugated molecule wire inserted decanethiol SAMs were prepared.

Preparation of the Conjugated Molecular Wire SAMs. The target conjugated molecular wire (1 mg) was dissolved in 5 mL of THF under nitrogen atmosphere; concentrated NH_4OH (5 μ L) was then added, and the mixture was incubated for 10 min to deprotect the thioacetyl group. After the Au substrate was immersed in the solution for 12–24 h in the absence of the light, it was rinsed with dry THF ultrasonically and dried under a nitrogen stream to give conjugated molecular wire SAMs.

Single Molecular Conductance by STM Break Junctions. STM break junctions were operated under ambient atmosphere using Au STM tips, following a modified procedure of Xu *et al.*¹³ Gold tips could penetrate into the SAM at -50 or -100 mV with current set-point in the range of 0.5–10 nA, and the Au–S bond was therefore formed. The feedback was then disabled, and the tip was lifted at a vertical rate of 4 nm/s while keeping the X – Y position constant. During the repeating vertical movement of the tip, the current was recorded as a function of the traveling distance. This procedure was repeated thousands of times for each sample, and statistical analysis was constructed to extract single molecular conductance from the staircase-like current–distance (I – S) curves.

CP-AFM Experiments. The CP-AFM experiments were performed at room temperature under ambient atmosphere on a Digital Instruments (Santa Barbara, CA) Nanoscope 3A Multimode equipped with an E-scanner and current sensitive attachment. Contact mode silicon cantilevers coated with Ti–Pt (MikroMasch, CSC21) were used. Ti–Pt conductive tip was in contact with SAMs as the top electrode, and the Au substrate served as the bottom electrode. Each I – V curve was recorded at an applied load of 2 nN using the same tip; I – V curves were collected at five different places for each SAM, and 5–10 measurements were conducted at each place.

Ultraviolet–Visible Spectroscopy. The ultraviolet–visible (UV–vis) absorption spectra were recorded from a Varian 50 Bio spectrometer at room temperature in THF with conventional 1.0 cm quartz cells.

Quantum Chemistry Computation. The electronic structures of the molecular wires were calculated by density functional theory ap-

proximation,³⁷ using the B3PW91 functional³⁸ coupled with the 6-311G(d,p) basis set³⁹ for OPE and LANL2DZ basis set⁴⁰ for OPERu, respectively.

Acknowledgment. This work was supported by the Natural Science Foundation of China (Grant No. 20225414). We gratefully thank anonymous reviewers for the insightful and helpful comments.

Supporting Information Available: Experimental details for the synthesis of OPERu and OPE, stochastic switching of OPE and OPERu, supplemental CP-AFM measurements for OPE and OPERu, and complete ref 37. This material is available free of charge via the Internet at <http://pubs.acs.org>.

REFERENCES AND NOTES

- Nitzan, A.; Ratner, M. A. Electron Transport in Molecular Wire Junctions. *Science* **2003**, *300*, 1384–1389.
- Tao, N. J. Electron Transport in Molecular Junctions. *Nat. Nanotechnol.* **2006**, *1*, 173–181.
- Lindsay, S. M.; Ratner, M. A. Molecular Transport Junctions: Clearing Mists. *Adv. Mater.* **2007**, *19*, 23–31.
- Mantooth, B. A.; Weiss, P. S. Fabrication, Assembly, and Characterization of Molecular Electronic Components. *Proc. IEEE* **2003**, *91*, 1785–1802.
- Xu, G. L.; DeRosa, M. C.; Crutchley, R. J.; Ren, T. *trans*-Bis(alkynyl) Diruthenium(III) Tetra(amidinate): An Effective Facilitator of Electronic Delocalization. *J. Am. Chem. Soc.* **2004**, *126*, 3728–3729.
- Flores-Torres, S.; Hutchison, G. R.; Soltzberg, L. J.; Abruna, H. D. Ruthenium Molecular Wires with Conjugated Bridging Ligands: Onset of Band Formation in Linear Inorganic Conjugated Oligomers. *J. Am. Chem. Soc.* **2006**, *128*, 1513–1522.
- Blum, A. S.; Ren, T.; Parish, D. A.; Trammell, S. A.; Moore, M. H.; Kushmerick, J. G.; Xu, G. L.; Deschamps, J. R.; Pollack, S. K.; Shashidhar, R. Ru₂(ap)₄(σ -oligo(phenyleneethynyl)) Molecular Wires: Synthesis and Electronic Characterization. *J. Am. Chem. Soc.* **2005**, *127*, 10010–10011.
- Kim, B.; Beebe, J. M.; Olivier, C.; Rigaut, S.; Touchard, D.; Kushmerick, J. G.; Zhu, X. Y.; Frisbie, C. D. Temperature and Length Dependence of Charge Transport in Redox-Active Molecular Wires Incorporating Ruthenium(II) Bis(σ -arylacetyl) Complexes. *J. Phys. Chem. C* **2007**, *111*, 7521–7526.
- Chen, F.; Hihath, J.; Huang, Z. F.; Li, X. L.; Tao, N. J. Measurement of Single-Molecule Conductance. *Annu. Rev. Phys. Chem.* **2007**, *58*, 535–564.
- Bumm, L. A.; Arnold, J. J.; Cygan, M. T.; Dunbar, T. D.; Burgin, T. P.; Jones, L.; Allara, D. L.; Tour, J. M.; Weiss, P. S. Are Single Molecular Wires Conducting. *Science* **1996**, *271*, 1705–1707.
- Cygan, M. T.; Dunbar, T. D.; Arnold, J. J.; Bumm, L. A.; Shedlock, N. F.; Burgin, T. P.; Jones, L.; Allara, D. L.; Tour, J. M.; Weiss, P. S. Insertion, Conductivity, and Structures of Conjugated Organic Oligomers in Self-Assembled Alkanethiol Monolayers on Au{111}. *J. Am. Chem. Soc.* **1998**, *120*, 2721–2732.
- Bumm, L. A.; Arnold, J. J.; Dunbar, T. D.; Allara, D. L.; Weiss, P. S. Electron Transfer through Organic Molecules. *J. Phys. Chem. B* **1999**, *103*, 8122–8127.
- Xu, B. Q.; Tao, N. J. Measurement of Single-Molecule Resistance by Repeated Formation of Molecular Junctions. *Science* **2003**, *301*, 1221–1223.

14. Beebe, J. M.; Kim, B.; Gadzuk, J. W.; Frisbie, C. D.; Kushmerick, J. G. Transition from Direct Tunneling to Field Emission in Metal–Molecule–Metal Junctions. *Phys. Rev. Lett.* **2006**, *97*, 026801-1–026801-4.
15. Seferos, D. S.; Blum, A. S.; Kushmerick, J. G.; Bazan, G. C. Single-Molecule Charge-Transport Measurements that Reveal Technique-Dependent Perturbations. *J. Am. Chem. Soc.* **2006**, *128*, 11260–11267.
16. Poirier, G. E. Characterization of Organosulfur Molecular Monolayers on Au(111) Using Scanning Tunneling Microscopy. *Chem. Rev.* **1997**, *97*, 1117–1127.
17. Donhauser, Z. J.; Mantooth, B. A.; Kelly, K. F.; Bumm, L. A.; Monnell, J. D.; Stapleton, J. J.; Price, D. W.; Rawlett, A. M.; Allara, D. L.; Tour, J. M.; et al. Conductance Switching in Single Molecules through Conformational Changes. *Science* **2001**, *292*, 2303–2307.
18. Moore, A. M.; Dameron, A. A.; Mantooth, B. A.; Smith, R. K.; Fuchs, D. J.; Cizek, J. W.; Maya, F.; Yao, Y. X.; Tour, J. M.; Weiss, P. S. Molecular Engineering and Measurements to Test Hypothesized Mechanisms in Single Molecule Conductance Switching. *J. Am. Chem. Soc.* **2006**, *128*, 1959–1967.
19. Ramachandran, G. K.; Hopson, T. J.; Rawlett, A. M.; Nagahara, L. A.; Primak, A.; Lindsay, S. M. A Bond-Fluctuation Mechanism for Stochastic Switching in Wired Molecules. *Science* **2003**, *300*, 1413–1416.
20. Moth-Poulsen, K.; Patrone, L.; Stuhr-Hansen, N.; Christensen, J. B.; Bourgoin, J. P.; Bjornholm, T. Probing the Effects of Conjugation Path on the Electronic Transmission through Single Molecules Using Scanning Tunneling Microscopy. *Nano Lett.* **2005**, *5*, 783–785.
21. Tsoi, S.; Griva, I.; Trammell, S. A.; Blum, A. S.; Schnur, J. M.; Lebedev, N. Electrochemically Controlled Conductance Switching in a Single Molecule: Quinone-Modified Oligo(phenylene vinylene). *ACS Nano* **2008**, *2*, 1289–1295.
22. Slowinski, K.; Chamberlain, R. V.; Bilewicz, R.; Majda, M. Evidence for Inefficient Chain-to-Chain Coupling in Electron Tunneling through Liquid Alkanethiol Monolayer Films on Mercury. *J. Am. Chem. Soc.* **1996**, *118*, 4709–4710.
23. Li, X. L.; He, J.; Hihath, J.; Xu, B. Q.; Lindsay, S. M.; Tao, N. J. Conductance of Single Alkanedithiols: Conduction Mechanism and Effect of Molecule–Electrode Contacts. *J. Am. Chem. Soc.* **2006**, *128*, 2135–2141.
24. Wold, D. J.; Frisbie, C. D. Fabrication and Characterization of Metal–Molecule–Metal Junctions by Conducting Probe Atomic Force Microscopy. *J. Am. Chem. Soc.* **2001**, *123*, 5549–5556.
25. Xiao, X. Y.; Nagahara, L. A.; Rawlett, A. M.; Tao, N. J. Electrochemical Gate-Controlled Conductance of Single Oligo(phenylene ethynylene)s. *J. Am. Chem. Soc.* **2005**, *127*, 9235–9240.
26. Haiss, W.; Wang, C. S.; Grace, I.; Batsanov, A. S.; Schiffrin, D. J.; Higgins, S. J.; Bryce, M. R.; Lambert, C. J.; Nichols, R. J. Precision Control of Single-Molecule Electrical Junctions. *Nat. Mater.* **2006**, *5*, 995–1002.
27. Huber, R.; Gonzalez, M. T.; Wu, S.; Langer, M.; Grunder, S.; Horhoiu, V.; Mayor, M.; Bryce, M. R.; Wang, C. S.; Jitchati, R.; et al. Electrical Conductance of Conjugated Oligomers at the Single Molecule Level. *J. Am. Chem. Soc.* **2008**, *130*, 1080–1084.
28. Liu, K.; Li, G. R.; Wang, X. H.; Wang, F. S. Length Dependence of Electron Conduction for Oligo(1,4-phenylene ethynylene)s: A Conductive Probe–Atomic Force Microscopy Investigation. *J. Phys. Chem. C* **2008**, *112*, 4342–4349.
29. Mayor, M.; von Hanisch, C.; Weber, H. B.; Reichert, J.; Beckmann, D. A *trans*-Platinum(II) Complex as a Single-Molecule Insulator. *Angew. Chem., Int. Ed.* **2002**, *41*, 1183–1186.
30. Schull, T. L.; Kushmerick, J. G.; Patterson, C. H.; George, C.; Moore, M. H.; Pollack, S. K.; Shashidhar, R. Ligand Effects on Charge Transport in Platinum(II) Acetylides. *J. Am. Chem. Soc.* **2003**, *125*, 3202–3203.
31. Simmons, J. G. Generalized Formula for the Electric Tunnel Effect between Similar Electrodes Separated by a Thin Insulating Film. *J. Appl. Phys.* **1963**, *34*, 1793–1803.
32. Young, R.; Ward, J.; Scire, F. Observation of Metal–Vacuum–Metal Tunneling, Field Emission, and the Transition Region. *Phys. Rev. Lett.* **1971**, *27*, 922–924.
33. Beebe, J. M.; Kim, B.; Frisbie, C. D.; Kushmerick, J. G. Measuring Relative Barrier Heights in Molecular Electronic Junctions with Ttransition Voltage Spectroscopy. *ACS Nano* **2008**, *2*, 827–832.
34. Mahapatro, A. K.; Ying, J.; Ren, T.; Janes, D. B. Electronic Transport through Ruthenium-Based Redox-Active Molecules in Metal–Molecule–Metal Nanogap Junctions. *Nano Lett.* **2008**, *8*, 2131–2136.
35. Kim, B.; Beebe, J. M.; Jun, Y.; Zhu, X. Y.; Frisbie, C. D. Correlation between HOMO Alignment and Contact Resistance in Molecular Junctions: Aromatic Thiols versus Aromatic Isocyanides. *J. Am. Chem. Soc.* **2006**, *128*, 4970–4971.
36. Reddy, P.; Jang, S. Y.; Segalman, R. A.; Majumdar, A. Thermoelectricity in Molecular Junctions. *Science* **2007**, *315*, 1568–1571.
37. Frisch, M. J. *Gaussian 03*, revision B.03; Gaussian, Inc.: Pittsburgh, PA, 2003.
38. Becke, A. D. Density-Functional Thermochemistry. 3. The Role of Exact Exchange. *J. Chem. Phys.* **1993**, *98*, 5648–5652.
39. Krishnan, R.; Frisch, M. J.; Pople, J. A. Contribution of Triple Substitutions to the Electron Correlation Energy in Fourth Order Perturbation Theory. *J. Chem. Phys.* **1980**, *72*, 4244–4245.
40. Hay, P. J.; Wadt, W. R. *Ab Initio* Effective Core Potentials for Molecular Calculations. Potentials for K to Au Including the Outermost Core Orbitals. *J. Chem. Phys.* **1985**, *82*, 299–310.